

MEASURING THE COSMIC WEB

Volker Müller¹, Kai Hoffmann², and Sebastián E. Nuza³

*Leibniz-Institut für Astrophysik Potsdam (AIP)
An der Sternwarte 16, D-14482 Potsdam, Germany*

¹ *vmueller@aip.de*

² *hoffmann@ice.cat*

³ *snuza@aip.de*

Received: 2011 July 10; accepted: 2011 XXX XX

Abstract. A quantitative study of the clustering properties of the cosmic web as a function of absolute magnitude and colour is presented using the SDSS Data Release 7 galaxy survey. Mark correlations are included in the analysis. We compare our results with mock galaxy samples obtained with four different semi-analytical models of galaxy formation imposed on the merger trees of the Millenium simulation. The clustering of both red and blue galaxies is studied separately.

Key words: Cosmology: observations – cosmology: theory – galaxies: statistics – large scale structure of the Universe

1. INTRODUCTION

The 200 years history of the Tartu Observatory is strongly linked with the exploration of the Earth and space at different scales. In the early 19th century, the triangulation along the Tartu Meridian Arc, 3000 km across Europe, helped to determine the size and precise shape of the Earth. First stellar parallax measurements (besides Bessel) by Wilhelm Struve, the founder of the Tartu Observatory, provided the basis for exploring our neighborhood within the Milky Way. The dynamical distance measurements of the Andromeda nebula and other *island universes* by Ernst Öpik in 1918–1922 opened the way to the first systematic works in the field of extragalactic astronomy.

The study of the large scale distribution of galaxies became an important research subject already over 50 years ago with the notion of filamentary structure as revealed by the Lick galaxy survey (Shane & Wirtanen 1954). The impression of a cellular structure of the Universe with dominance of filaments and large voids in the galaxy distribution was developed during the period 1974–1980 at the cosmology school of Tartu Observatory (Joeveer, Einasto & Tago 1978; Einasto, Joeveer & Saar 1980). These results were presented at the IAU Symposium No. 79 at Tallinn (Longair & Einasto 1978) where an exposition of the pancake theory of large scale

structure formation was presented by Zel'dovich, Doroshkevich, Shandarin, Sigov and Kotok (see e.g. Zel'dovich 1978). Already at this time, galaxy formation in proto-clusters was discussed by Doroshkevich, Saar & Shandarin (1978).

A quantitative description of the galaxy clustering was provided for the first time by Totsuji & Kihara (1969) establishing the power law dependence of the angular auto-correlation function. However, the true spatial distribution became obvious only with the advent of the Harvard-Smithsonian Center for Astrophysics redshift surveys (Huchra et al. 1983; Geller & Huchra 1989). The quantitative properties of the spatial clustering were provided by Davis & Peebles (1983) and Efstathiou & Jedrzejewski (1984). Later, more extended surveys confirmed the power law behaviour of the correlation function, in particular the Automatic Plate Measuring survey (Efstathiou 1993); the Las Campanas Redshift Survey (Tucker et al. 1997); the Two-degree-Field Galaxy Redshift Survey (Madgwick et al. 2003), and the Sloan Digital Sky Survey (Li et al. 2006, Swanson et al. 2008). In these and related studies it was shown that the clustering of galaxies strongly depends on their magnitudes, morphological types, and colours (e.g. Davis & Geller 1976; Loveday et al. 1995; Zehavi et al. 2010).

We have been involved in a detailed analysis of the cosmic web using both modern redshift surveys and numerical simulations of galaxy formation together with colleagues from Tartu. Building on standard techniques such as those used in Tucker et al. (1997) we analyze here the largest SDSS galaxy redshift catalogue presently available. We also present an analysis of mark correlation functions. The aim of this contribution is to investigate the distribution of galaxies and its relation to the underlying dark matter density field within the standard Λ CDM paradigm. We perform a correlation analysis depending on the absolute magnitude and colour of observed galaxies and compare the results with a series of semi-analytical models of galaxy formation imposed on the Millenium simulation (Springel et al. 2005).

2. DATA AND MOCK SAMPLE SELECTION

We study the cosmic web using the SDSS Data Release 7, the largest near field galaxy redshift survey available. The survey is complete and comprises a large contiguous region of the Northern Galactic cap with 7500 deg^2 . Photometric calibration and k -correction to redshift $z = 0$ is done according to Hogg et al. (2002) using the galactic extinction measurements of Schlegel et al. (1998). We employ absolute Petrosian (1976) AB-magnitudes and use the New York University Value-Added Galaxy Catalog (Blanton et al. 2005).

Starting from the observed R -band magnitude and redshift distributions, we define two sets of volume-limited galaxy samples as illustrated in Fig. 1 (see Table 1). The first set of volume-limited samples (m1 to m12) is used to investigate the dependence of the auto-correlation function on absolute magnitude. The samples are selected in order to cover a large magnitude range and to enclose a sufficient number of galaxies for the analysis. Therefore, the samples partially overlap, each separate sample contains however a significant number of independent objects to derive the auto-correlation functions. The second set (r1, r2, r3) was selected to cover a large range of magnitudes. This allows us to investigate the magnitude dependence of clustering using mark correlation functions. We impose a subdivision into red and blue galaxies applying least squares fitting through the green valley in the $U-R$ and R plane, which leads to a separation line $U-R = 1.8 - 0.05 \times (R+19)$.

For comparison we use four sets of mock galaxy samples constructed using

Table 1. Properties of the SDSS volume-limited samples. The correlation length, r_0 , of the different samples is given for samples m1 – m12 (for blue galaxies only m1 – m7).

Sample	R_{low}	R_{up}	z_{low}	z_{up}	Number	Red	Blue	$r_0(\text{all})$	$r_0(\text{red})$	$r_0(\text{blue})$
m1	-18.35	-19.86	0.020	0.056	42 165	17 801	24 364	6.33	8.72	4.58
m2	-19.08	-20.43	0.026	0.078	86 272	45 531	40 741	6.45	7.83	4.81
m3	-19.73	-20.94	0.032	0.105	129 802	79 097	50 705	7.29	8.35	5.36
m4	-20.28	-21.40	0.040	0.136	161 913	107 837	54 076	7.49	8.26	5.65
m5	-20.76	-21.82	0.049	0.169	161 392	114 573	46 819	8.22	8.85	6.16
m6	-21.16	-22.20	0.058	0.20	172 264	94 975	32 289	8.94	9.74	6.99
m7	-21.49	-22.54	0.068	0.20	69 787	55 468	14 419	9.07	9.60	7.70
m8	-21.77	-22.86	0.078	0.20	32 677	27 432	5 245	10.11	10.50	
m9	-21.98	-23.16	0.090	0.20	15 545	13 597	1 948	11.40	11.79	
m10	-22.15	-23.43	0.102	0.20	8 343	7 483	860	12.07	12.45	
m11	-22.26	-23.70	0.116	0.20	5 077	4 614	463	12.81	13.05	
m12	-22.36	-23.96	0.130	0.20	3 120	2 856	264	13.29	13.70	
r1	-18.51	-20.77	0.03	0.06	63 546	31 464	32 082			
r2	-19.39	-22.28	0.06	0.09	125 491	76 733	48 758			
r3	-20.01	-23.16	0.09	0.12	114 266	74 612	39 654			

the Millenium simulation. It follows the evolution of dark matter haloes and sub-haloes using 2160^3 particles in a large box of $500 h^{-1}$ Mpc length on a side. Galaxy catalogues are modeled using semi-analytical models of galaxy formation from merger trees of haloes in the simulation. The model of Croton et al. (2006, hereafter C06) implements AGN feedback in two channels to efficiently suppress star formation in high mass haloes (‘quasar’ and ‘radio’ modes), thereby forming a realistic population of elliptical galaxies. The model of De Lucia & Blaizot (2007, hereafter D07) builds on the first model and improves the treatment of satellite mergers, using a more realistic dust model and a different initial mass function for the stellar population synthesis. The third catalogue of mock galaxies, produced by Font et al. (2008), includes a modelling of ram pressure stripping of satellite galaxies by hot gas inside large dark matter haloes. In this way, the luminosity function of faint red galaxies is better reproduced. Finally, the model of Guo et al. (2011, hereafter G11) improves the treatment of the cooling flow regime and the rapid gas inflow, and it updates some parameters related with star formation and feedback processes. The mock galaxy samples are constructed applying the same angular selection as in the observations as well as the magnitude and redshift ranges provided in Table 1.

3. CORRELATION ANALYSIS

The correlation functions are evaluated using the Landy & Szalay (1993) estimator. Data-data, data-random and random-random pairs are generated with the same angular selection function of observations and the redshift bounds given in Table 1, however not taking into account the fiber separation limit of the SDSS. The estimator reads as follows

$$\xi(r) = \frac{\langle DD(r) - 2DR(r) + RR(r) \rangle}{\langle RR(r) \rangle}.$$

Errors are estimated using 10 bootstrap resamplings of the data. Fig. 2 shows the

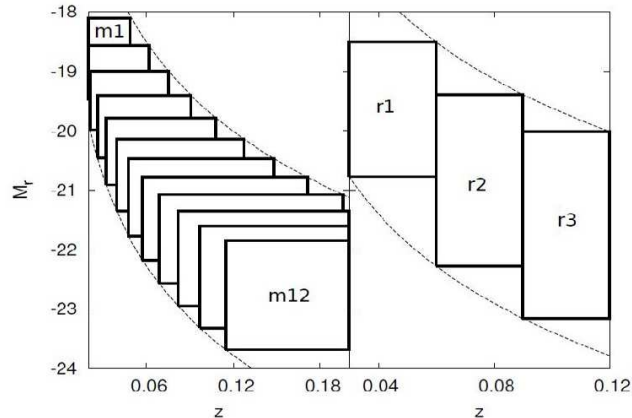


Fig. 1. Magnitude and redshift boundaries of the 12 (left panel) and 3 (right panel) volume-limited galaxy samples for a large coverage in depth (m samples) and magnitude (r samples), respectively.

convex form of the correlation function over the range from $0.2 - 50 h^{-1}$ Mpc. The solid line in the left panel shows the result corresponding to all galaxies for the sample m1. Additionally, a power law fit at the correlation length scale, i.e. where $\xi(r) = 1$, is also shown. The dashed line stems from red galaxies and lies about 0.2 dex above that of the full galaxy sample, the dot-dashed line stems from blue galaxies lying about 0.15 dex below. The slope of the power law is about $\gamma \cong 1.4$ for all samples. For the remaining datasets we get similar results, however, the difference of the clustering strength between red and blue galaxies gets smaller as magnitudes increase.

The right panel of Fig. 2 shows the ratio between the full correlation functions of the sample m4 and all four mock catalogues. For clarity, error bars are only given for the upper and lower curves. The correlation functions of models C06 (solid line) and G11 (dot-dashed line) reproduce the shape of the observed correlation function over almost all spatial scales. However, the clustering amplitude is underpredicted by about 20 percent. Acceptable results are also obtained for the model D07, while F08 overpredicts the clustering of close pairs by up to a factor of two. The correlation function of other samples behave in a similar way.

The results can be described in a compact form evaluating the change of the correlation length as a function of absolute magnitude. The left panel of Fig. 3 shows the correlation length for the mean absolute R -magnitudes of samples m1 to m12. The solid, dashed and dot-dashed lines correspond to all, red, and blue galaxies, respectively. The correlation length difference between red and blue galaxies decreases from about $4 h^{-1}$ Mpc at $R = -18.4$ to $2 h^{-1}$ Mpc at $R = -21.5$. As seen in the figure, the brighter samples are dominated by red galaxies. The right panel shows the results corresponding to the G11 model. The correlation lengths of all and blue galaxies stay nearly constant between $R = -18.4$ and $R = -21$, while the correlation length of red galaxies decreases. This is due to the large number of satellites present among faint galaxies (cp. also Weinmann et al. 2006) that tend to cluster more strongly than field red galaxies with $R \cong -21$. At brighter magnitudes the correlation length increases due to the higher bias of more

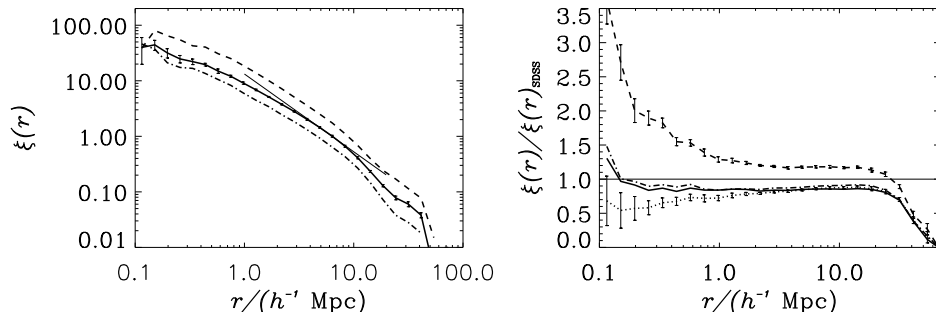


Fig. 2. *Left:* Two-point auto-correlation function for sample m1 with all galaxies (solid line), red galaxies (dashed line) and blue galaxies (dot-dashed line). For the full sample, a power law fit, $\xi = (r/r_0)^{1.4}$, centered at the correlation length scale, r_0 , is shown. Error bars for the full sample are partly smaller than the line thickness. *Right:* Ratio between model correlation functions and SDSS galaxies for the m4 sample. The different semi-analytic mock samples considered are those of C06 (solid line), D07 (dotted line with error bars), F08 (dashed line with error bars), and G11 (dash-dotted line).

massive haloes with respect to the underlying mass distribution. The remaining semi-analytical models display similar trends.

The ratio between the observed correlation length of red and blue galaxies and those corresponding to the semi-analytical models considered here can be seen in Fig. 4 (left and right panels respectively). In general, most models can explain the clustering amplitude of galaxies as measured by the correlation length with about 20 percent accuracy. However, there is a general trend for bright blue galaxies to be too weakly clustered. This is probably due to the fact that massive haloes display a too efficient star formation which therefore appear too bright for a given clustering strength. The trend showed by red galaxies is in principle similar. A remarkable exception can be seen at the faintest magnitude bin due to the efficient feedback implemented in the models. The other important exception is the increase observed for $R \lesssim -21$ in model C06 which is due to the strong quasar feedback implemented that makes bright red galaxies to be hosted by too massive and, therefore, too strongly clustered haloes.

4. MARK CORRELATION FUNCTION

The trends already discussed for the clustering amplitude of galaxies using the standard two-point correlation function can be further investigated by means of the mark correlation function (e.g. Beisbart, Kerscher & Mecke 2002). This statistical estimator is defined as the average of the inner galaxy properties m – here taken as color index $U - R$ or R magnitude – as a function of separation r and can be written as ($\langle m \rangle$ is the average over the mark on the whole sample)

$$k_m(r = |r_1 - r_2|) = \frac{\langle m(r_1) + m(r_2) \rangle}{2\langle m \rangle}.$$

The left panel of Fig. 5 shows the mark correlation function of the samples m1 and m6 (solid and dashed lines respectively) compared to the corresponding mock

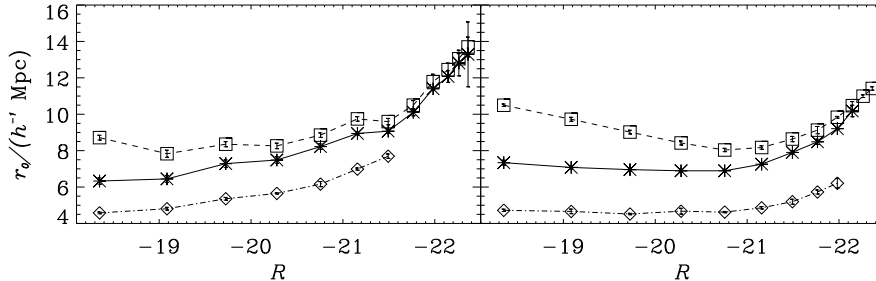


Fig. 3. Correlation length as a function of mean R -magnitude. *Left:* SDSS samples from m1 to m12 for all galaxies (stars and solid line), red galaxies (open squares and dashed lines), and blue galaxies (open diamonds and dash-dotted line). *Right:* idem as left panel but for mock samples in the G11 model. Error bars represent 2 standard deviations, they are smaller than the symbols.

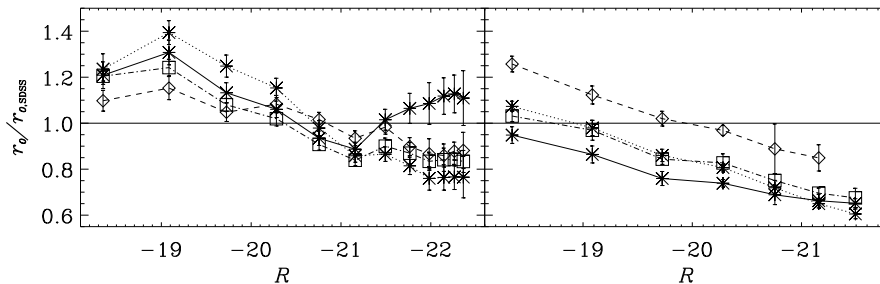


Fig. 4. Ratio of the correlation length of mock and SDSS data as a function of mean R -magnitude. *Left:* m1 to m12 samples for red galaxies. *Right:* m1 to m7 samples for blue galaxies. The different semi-analytic mock samples considered are those of C06 (asterisks and solid line), D07 (asterisks and dotted lines), F08 (open diamonds and dashed line) and G11 (open squares and dot-dashed line). Errors are again 2 standard deviations.

samples for model F08 (dotted lines) using $U - R$ colours as a mark. Interestingly, there is a significant signal over a distance of about $10 h^{-1}$ Mpc where the samples show redder $U - R$ colours than the average. For the smaller scales this enhancement is about 0.05 to 0.1 mag. The excess of red neighbours is the result of the morphological transformation of galaxies by direct and tidal interactions. Since this effect is much stronger for faint galaxies it is natural to find a higher signal for sample m1. Below $1 h^{-1}$ Mpc our mock galaxies show a too strong mark correlation function. Obviously, the suppression of star formation in close galaxy pairs is overestimated in the models. The same behaviour is seen for the other mock samples.

As can be seen in the right panel of Fig. 5 when using absolute magnitudes as a mark the resulting signals are much weaker. The correlations for the samples r1 and r3 are shown as solid and dashed lines, while measures below and above $k_{U,R} = 1$ correspond to U - and R -bands, respectively. This means that close pairs

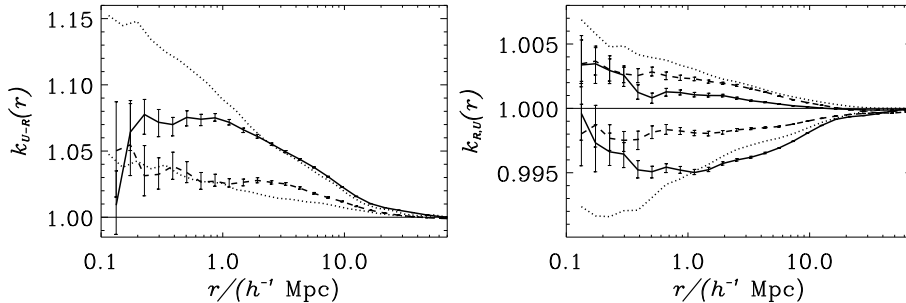


Fig. 5. *Left panel:* Mark correlation function using the $U - R$ colour as mark for samples m1 (solid line) and m6 (dashed line) in comparison with mock samples given by the F08 model (dotted lines). *Right:* Mark correlation function using the U -band ($k_U < 1$) and R -band ($k_R > 1$) absolute magnitudes as mark for samples r1 (solid line) and r3 (dashed line) in comparison with mock samples given by the F08 model (dotted lines). For clarity, mock galaxies here are only compared with sample r1. Errors are one standard deviation.

with a separation up to $10 h^{-1}$ Mpc are brighter in the R band and dimmer in the U band by less than 0.005 mag. Despite the fact that the effect is weak, the result is significant as the corresponding error bars show. In this case errors are estimated using 100 samples with randomly reshuffled marks.

3. DISCUSSION

The clustering of SDSS galaxies was previously discussed by Zehavi et al. (2010) mainly using the angular correlation function. Although this approach has the advantage of being independent of redshift space distortions, it uses only part of the information encoded in the galaxy distribution. However, results concerning the colour and magnitude dependence of clustering are similar to ours. Interestingly, the clustering of faint galaxies with $R \gtrsim -21$ is only weakly dependent on magnitude. In contrast, brighter galaxies are increasingly strongly clustered as clearly seen from the luminosity dependence of the correlation function.

We compared the clustering of SDSS galaxies with a large set of model galaxy samples based on the merger trees of the Millenium simulation that assume different semi-analytical prescriptions for galaxy formation models. These different theoretical models are able to qualitatively reproduce the clustering dependence as a function of magnitude and colour. However, quantitatively, still there exist significant differences, with the F08 model showing the smallest discrepancies for scales above $1 h^{-1}$ Mpc.

In addition to the standard two-point correlation technique, we carried out a new analysis using mark correlation functions which is suitable to assess the strength of galaxy transformations linked to their formation process. Surprisingly, we found a significant signal for galaxy pairs with a separation up to $10 h^{-1}$ Mpc depending on colour, and to a weaker extent, on absolute magnitudes.

It is our plan to continue the study of the properties of the galaxy distribution and its connection with the large scale density field using mark correlation techniques. To characterize the density field we combine cosmological simulations with

a galaxy group catalog to get the positions of suspected dark matter haloes. In extrapolating the mass density into the zones of influence of each halo we estimate the fine scale density field that reproduces both, the observed large scale galaxy distribution, and the average density profile around each group (Muñoz, Müller & Forero-Romero 2011). This approach will therefore allow to further investigate the relation between the galaxy properties and their environmental density aiming at improving our knowledge of the cosmic web.

ACKNOWLEDGMENTS. VM is grateful to the organizers of the conference ‘Expanding the Universe’ for the invitation and hospitality. SEN acknowledges support by the Deutsche Forschungsgemeinschaft under the grant MU1020 16-1.

REFERENCES

- Beisbart C., Kerscher M., & Mecke K. 2002, *Lecture Notes in Physics*, 600, 358
- Blanton M. R., Schlegel D. J., Strauss M. A. et al. 2005, *ApJ*, 129, 2562
- Croton D. J., Springel V., White S. D. M. et al. 2006, *MNRAS*, 365, 11
- Davis M., Geller M. J. 1976, *ApJ*, 208, 13
- Davis M., Peebles P. J. E. 1983, *ApJ*, 267, 465
- De Lucia G., Blaizot J. 2007, *MNRAS*, 375, 2
- Doroshkevich A. G., Saar E. M., & Shandarin S. F. 1978, *Proceedings of the IAU Symposium: Large Scale Structures in the Universe*, 79, 423
- Efstathiou G. 1993, *Proceedings of the National Academy of Science*, 90, 4859
- Efstathiou G., Jedrzejewski R. I. 1984, *Adv. Space Res.*, 3, 379
- Einasto J., Joeveer M. Saar, E. 1980, *MNRAS*, 193, 353
- Font A. S., Bower R. G., McCarthy I. G. et al. 2008, *MNRAS*, 389, 1619
- Geller M. J., Huchra J. P. 1989, *Science*, 246, 897
- Guo Q., White S. Boylan-Kolchin M. et al. 2011, *MNRAS* 413, 101
- Huchra J., Davis M., Latham D., Tonry J. 1983, *ApJS*, 52, 89
- Li C., Kauffmann G., Jing Y. P. et al. 2006, *MNRAS* 368, 21
- Joeveer M., Einasto J., Tago E. 1978, *MNRAS*, 185, 357
- Longair M. S., Einasto J. 1978, *Proceedings of the IAU Symposium: Large Scale Structures in the Universe*, 79
- Loveday J., Maddox S. J., Efstathiou G., Peterson, B. A. 1995, *ApJ*, 442, 457
- Madgwick A. S., Hawkins E., Lahav O. 2003, *MNRAS* 344, 847
- Muñoz J. C., Müller V., Forero-Romero J. E., 2011, *MNRAS* in press, arXiv:1107.1062
- Peebles P. J. E., Hauser M. G. 1974, *ApJS*, 28, 19
- Shane C. D., Wirtanen C. A. 1954, *ApJ*, 59, 285
- Springel V., White S. D. M., Jenkins A. et al. 2005, *Nature*, 435, 629
- Swanson M. E. C., Tegmark M., Hamilton A. J. S., Hill J. C. 2008, *MNRAS* 387, 1391
- Totsuji H., Kihara T. 1969, *PASJ* 21, 221
- Tucker D. L., Oemler Jr. A., Kirshner R. P. et al. 1997, *MNRAS*, 285, L5
- Weinmann Simone M., van den Bosch Frank C. et al. 2006, *MNRAS* 372, 1161
- Zehavi I., Zheng Z., Weinberg D. H. et al. 2010, arXiv 1005.2413
- Zel’dovich Ya. B. 1978, *Proceedings of the IAU Symposium: Large Scale Structures in the Universe*, 79, 409